FATIGUE FRACTURE ASSESSMENT OF HIGH STRENGTH STEEL USING THERMOGRAPHIC ANALYSIS

M. Somers[1], S. Chhith[1,2], W. De Waele[1] and R. H. Talemi[3]

[1] Ghent University, Laboratory Soete, Belgium
[2] Flanders Make, The Strategic Center for the Manufacturing Industry, Belgium
[3] Arcelor Mittal Global R&D Gent-Ocas N.V., Belgium

Abstract: Fatigue behaviour is most commonly evaluated in uni-axial cyclic stress tests using standardised dog-bone samples. When components are sharply bent into shape and subjected to cyclic loading, the fatigue damage will accumulate at the inside of the bend. This paper reports on an experimental investigation about the feasibility of infrared thermographic techniques to monitor fatigue damage initiation and accumulation. By monitoring spectral components of the thermal response, the fatigue limit, the onset of crack initiation and the ratio of initiation to propagation lifetime can all be determined. Also the effect of surface treatments on initiation properties is investigated. Most results are consistent with expected behaviour based on a previous study, indicating that thermographic techniques have a greater sensitivity and can be used to reduce the number of samples and time required for fatigue characterisation.

Keywords: Fatigue; Thermography; Bending; High Strength Steel

1   INTRODUCTION

In modern, large scale industrial applications the use of high strength steel is becoming more commonplace [2]. This has allowed for thinner wall sections in an effort to reduce weight in heavily loaded structures. In order to avoid welds, which are prone to defects, bending can be used as an alternative manufacturing method. Components that are designed with bent sections are burdened with stress-concentrations of greater intensity. In applications like crane arms and high pressure vessels the loads are large and slowly cycling. All of this results in low cycle fatigue occurring under the multi-axial stress state at the inside of bend. As this fatigue type results in large plasticity near the crack tip, thermography is proposed to detect the expected energy dissipation phenomenon. Most related studies have focussed on mild steel using standardized dog-bone samples [3],[9], or welded connections [5]. The goal of this study is to evaluate the feasibility of the infrared method to determine the fatigue properties of HSS bent samples. IR thermography is used to determine the fatigue limit of a bent sample compared to that of the undeformed material and quantify the timings of crack initiation and propagation stages. In a preceding study [1] the bending process of HSS samples and their fatigue resistance have been evaluated by finite element simulations and experimentally tested. The resulting FEA model has also been used to simulate the stress concentration at the bend root. A Whöler curve has been created and fatigue related material constants have been characterized with standard dog-bone samples. A crack initiation criterion for fatigue tests on bent samples was first defined to be 0.1mm displacement after initial stabilization. This resulted in an estimated initiation life at 80% of the total fatigue life with cracks of 0.64mm deep found. In order to increase sensitivity, IR thermography was attempted. The thermographicy technique has shown to provide data with clearly defined phases (Figure 1) that are in line with descriptions found in literature [3]. This reduced the estimation of the initiation life to about 55% of the total fatigue life.
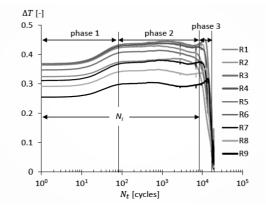

Figure 1. Temperature amplitude measured during fatigue test [1]

2   INFRARED THERMOGRAPHY FOR FATIGUE EVALUATION

2.1   Fatigue

Components that are subjected to varying loads are at risk of developing cracks. The evolution of these cracks can be separated in 3 different stages; damage accumulation, initiation and propagation until final fracture [4].

Assuming an initial ideally smooth surface without significant local stress raisers, under cyclic loading with magnitude below the yield strength, the seed of a growing crack can still be formed. Micro-plastic movement of the crystal lattice along a preferred plane will take place at the surface, where plastic constraint is minimal, if the maximal load is high enough. Upon releasing this load, a microscopic ridge or valley acting as a stress concentration is left. This damage accumulates and will start to grow into an intiating crack. If the maximum load does not cause micro-plasticity no crack will grow. The material has infinite fatigue life and the global stress level is called the "Fatigue Limit" of the material.

When sufficient damage has accumulated at the same location, it becomes more accurate to consider it as a microscopic crack. During this phase the standard fatigue cycle crack growth starts to apply and the crack grows to the size of a few grains. Along its path the crack will have to cross grain boundaries, which are relatively significant barriers for the size of the crack at this moment. In these regions the crack can be arrested if the load is too low, also granting the material theoretically infinite fatigue life.

When the initiated crack grows large enough the fatigue properties no longer depend on the microstructure near the surface. Instead the bulk material properties will govern the crack-growth. During this phase the crack front moves deeper into the sample, until its cross-section is reduced so much that the maximum load causes a static overload failure.

2.2   Infrared thermography

IR thermography is based on detecting the infrared radiation emitted by the sample under investigation with a specialized digital camera. The technique used here relies on the energy fed to the sample by loading, so it is a form of active thermography. It allows to create a thermal image of all objects within the field of view. At each point in a region of interest the temperature can thus be recorded for the duration of a test.

Temperature is related to the stress-strain response of the loaded material [5]. In fatigue tests the applied load is sinusoidal, so equation 1 shows the form of the Fourier decomposition of the thermal response [6]. In the elastic range the temperature is linearly related to the applied stress, represented by T1. When the sample is under tensile stress, temperature drops and the reverse occurs under compressive stress. Equation 2 shows this relation of temperature amplitude to the sum of stress components [7]. This means the effect does not change the average sample temperature. This thermoelastic coupling component follows the sinusoidal load with angular speed ω directly and has a phase shift φ_1. As soon as the material starts to plastically deform, the hysteresis energy dissipation increases local average temperature. This plastic dissipation effect is represented by T2 in the equation 1 and is shown to oscillate at twice the loading frequency with its own phase shift φ_2 [1]. More spectral components of the temperature can be considered but are too small to be included in the analysis of these fatigue experiments. The final term LD(t), linear drift, represents the gradual heat-up of the entire sample due to the plastic dissipation until it's in thermal equilibrium with the environment.

$$T_{meas} = LD(t) + T_1 \sin(\omega t + \phi_1) + T_2 \sin(2\omega t + \phi_2) + \dots \tag{1}$$

$$\Delta \sigma_{kk} = -k T_1 \tag{2}$$

The values of T1 and T2 are expected to be correlated with physical phenomenon that signify different fatigue phases. In order to obtain data that can give accurate results, 10 images are taken during each load cycle, well above the theoretical minimum of images [8]. When the test is monitored on-line, the load is applied at 5Hz and the camera records at 50Hz. If the data is post-processed, the camera can record at 100Hz so the load frequency is 10Hz. The temperature data is recorded on a computer and every set of 1024 points is processed by FFT to determine its spectrum like the one in Figure 7. From this spectrum the first harmonic T1 is found by taking the global maximum amplitude from the spectrum. This simple calculation can be performed on-line. The second harmonic T2 is found by searching the local maximum near twice the frequency of the first harmonic. This increases the computational complexity interrupting data acquisition software and is too slow to be monitored on-line.

3   EXPERIMENTAL STUDY

3.1   Materials and specimens

The material used in this test is steel grade S700MC, a thermo-mechanically hot rolled low carbon steel. From a previous study the yield strength of the material was found to be 841MPa, the tensile strength equals 885MPa [1]. The fatigue limit corresponding to minimal 2e6 cycles has been estimated at 570MPa.
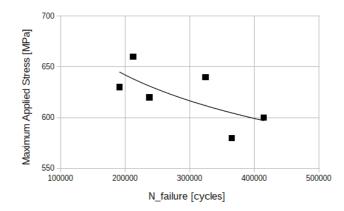

Figure 2. Whöler curve S700MC

Since the goal of the study is to determine the effect of bending manufacturing steps on the fatigue behaviour of components, bent samples were designed in a preceding study [1]. In order to ensure plain strain conditions the samples are extra wide and narrowed at the root of the bend to concentrate stress in that region. In order to fit with the clamps of the test-bench the ends were also narrowed, but this did not change the failure locus as the stress concentration in the bend is still dominant.
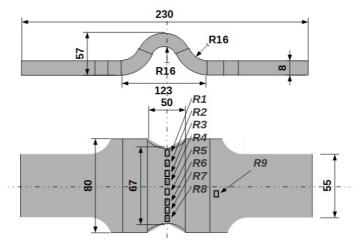

Figure 3. Sample geometry, adapted to fit clamps, dimensions in mm

A finite element model has been adopted from a previous study [1] and was used to get a qualitative idea of the stress concentrations. The model has a mesh of approximate size 0.75mm and boundaries conditions so the ends can only move in the lengthwise direction. As seen in Figure 4 a uniform applied load of 24MPa resulted in a maximum stress of 612MPa located just off-centre in the root of the bend at the points R3 and R6. Due to the elastic-plastic material model these maximum stress values do not scale linearly with the load applied and are calculated individually.
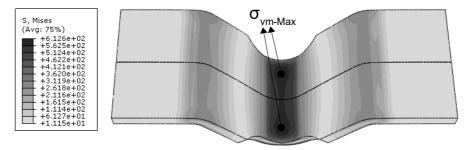

Figure 4. FEA von Mises stress indicating off-centre maximum stress concentration at 30kN

Some of the samples have received surface treatments (Figure 5) in unbent conditions at the region of the bend. At the root of the bend, ridges and valleys of a few millimetres high, created during the bending process, span the entire width of the untreated samples. As this surface quality may affect the fatigue performance, a pre-bending grinding or peening operation has been applied to some samples. It is expected that these increase the fatigue limit and the initiation life.
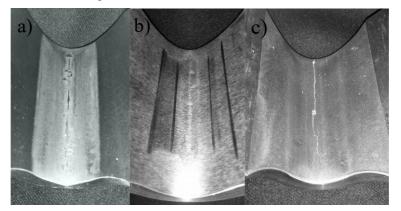

Figure 5. Surface treatments: a) standard, b) ground, c) peened (photograph after complete fatigue failure)

3.2   Experiments

3.2.1   Setup

The fatigue tests are performed by mounting a pair of bent samples, welded together at the top and bottom, in an ESH 100kN servo hydraulic test-bench. The sinusoidal loads are applied by force control through the clamps at a consistent fatigue load ratio R=0.1 in each of the tests.
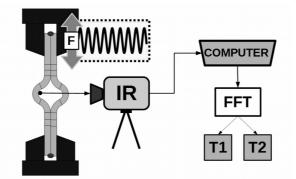

Figure 6. Schematic drawing of the experimental setup

In order to maximise the thermal radiation and reduce unwanted reflections, the surface of the specimen the IR camera is pointing at is painted black. The camera is positioned at a distance of around 0.2m and has a lens mounted with appropriate focal distance range. Images are taken of the entire width of the sample at the bend and the data is reduced to a series of averages in small rectangular zones of interest (as seen in Figure 3).

Three different types of experiments are performed, each intending to link a different temperature effect to a specific fatigue phenomenon.

3.2.2   Fatigue limit

The test to determine the fatigue limit is based on detecting the plastic dissipation of damage accumulation at the surface of uncracked samples and equating this to the presence of significant T2 values. The sample is loaded with stepwise increasing stress amplitude for 2000 cycles per step. This means the total duration of the test is much lower than the conventional Whöler-curve technique of running for millions of cycles to failure at several stress levels. It is even faster than the thermographic method reported on in [9], based on detection of temperature deviations and requiring 15,000 cycles per step. For the type of test used in this study a higher loading frequency results in less noise on the T2 signal (as shown in Figure 8); therefore 10Hz is applied here. This technique has been fine-tuned on a dummy sample and then validated on a second. This final test ran from 5 to 25kN in steps of 5kN, or expressed in maximum von Mises stress, from 110 to 500MPa respectively on a sample without surface treatment.
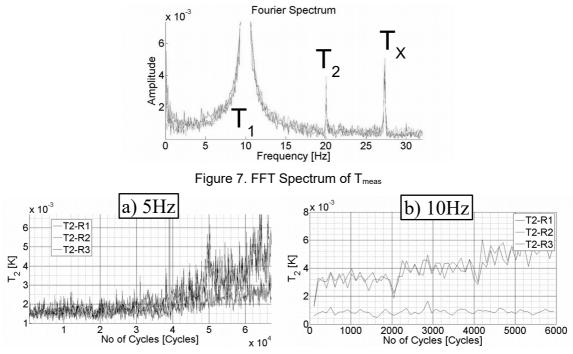
Figure 7. FFT Spectrum of T_{meas}

Figure 8. Comparison of the T2 noise for a) 5Hz load and b) 10Hz load

3.2.3 Crack initiation

Determining the end of initiation is done by measuring T1 on-line and terminating the fatigue load when this value starts deviating at one of the zones of interest. This position is then marked on the surface of the sample for locating the crack using microscopy. After that, the sample is cut perpendicular to the monitored surface and embedded in bakelite (see Figure 9) to measure the detected crack depth using a SEM microscope. If T1 increases in one of the zones of interest the crack is expected to initiate inside the selected region. The stress concentration of the crack maximises the local stress range and therefore the linear elastic temperature response amplitude. If T1 decreases a crack could have initiated in close proximity yet outside the zone of interest because the crack diverts the applied stress from the surface nearby. This method was evaluated on 2 samples with different surface treatments. Each subjected to a maximum load of 40kN (corresponding to 815MPa at the bending root) with R=0.1 stress ratio. The results will be compared to the initiation test of the previous study.
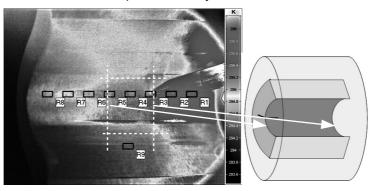

Figure 9. Marking the deviating zone of interest and extracting microscopy samples

3.2.4 Full fatigue failure

In this test the sample is loaded until it completely fails due to the reduction of the cross-section as the crack grows (see Figure 5.c)). By using the same criterion as the crack initiation test, the ratio of initiation to propagation can be calculated. After this point, the T1 signal will drop rapidly in all regions as the crack front moves into the sample and less IR radiation reaches the camera. After the failure test the sample is embrittled by freezing the samples and breaking them open so the crack surface can be analysed. This test has been performed 3 times at different stress levels, 610MPa, 815MPa and 855 MPa (respectively resulting from 30, 40 and 50kN applied to the total sample).

4   RESULTS & DISCUSSION

4.1   Fatigue Limit

In the resulting temperature data of this test the load steps are distinct and in T2 a jump in magnitude clearly indicates the fatigue limit. As shown in Figure 10 T2 is still low in step 2, "10kN", but significantly higher in the next step, "15kN" indicating local damage accumulation. This means that the actual fatigue limit is somewhere between 200 and 325MPa.
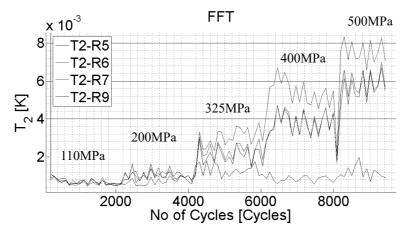

Figure 10. Fatigue limit test T2

This stress window can be narrowed by redoing the test with smaller load steps in the range of 200 to 300 MPa. This already shows that the bending process strongly reduces the fatigue limit (as the undeformed material was at 570MPa) possibly due to the inferior surface quality of the untreated bent sample.

In Figure 7 both T1 and T2 are detected at respectively the loading frequency 10Hz and twice the loading frequency 20Hz. However in all tests a peak at 27Hz also appeared. In 5Hz tests it was detected at 23Hz (due to the FFT mirror over 25HZ). Currently, the authors have no physical explanation for this observation. However, this does not seem to affect the thermal data and is therefore ignored in further analysis.

4.2   Crack Initiation

This test shows that after an initial stabilisation period the bulk of the zones of interest show T1 values that remain parallel to each other. In the ground sample T1 is rising at R3 so a crack is expected to initiate inside the selected box. The test was stopped after about 11000 cycles. In the peened sample R6 drops first so a crack will be growing slightly outside the box. This test was stopped after 10500 cycles. These off-centre positions correspond to the points of maximum von Mises stress that the finite element model (in Figure 4) predicted. These results are around the same number of cycles as the previous study with standard samples. Since the samples here have been surface-treated, which would improve the lifetime, the detected cracks should be smaller. This can indeed be seen on the fractography in Figure 12.
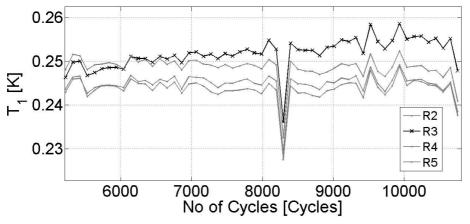

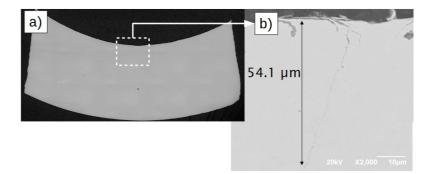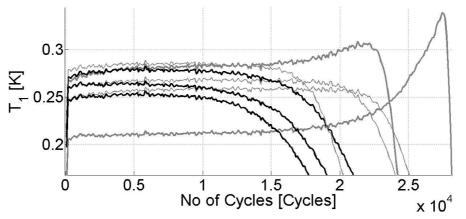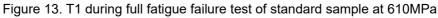Figure 11. Stabilized T1 during test of ground sample

Figure 12. SEM crack-size peened sample

The SEM images reveal that the test with the peened sample stopped at a crack size of 54µm, which is a factor 10 smaller than in a previous study [1]. These small cracks correspond to the early initiation detection of the treated samples. This increased sensitivity does mean the T1 deviation needs to big enough to be declared initiating as no discernible crack was found in the sample from Figure 11.

4.3   Full Fatigue Failure

For these tests the first part is the same as the initiation test. As before the first initiation points are off-centre, followed by multiple initiation points widening the crack front. When most of the width of the sample contains initiated cracks, the propagation phase begins and all T1 values drop sharply. As soon as the cross-section has decreased enough, each maximal loading cracks the sample further. This sudden tensile overload fracture audibly pops until the increasing displacement of the clamps triggers the test-bench. The initiation of the peened sample at 815MPa ended around 10000 cycles with dropping T1 at R3, this is 50% of the total 20.000 cycles lifetime. For the tests with the standard surfaces some of the T1 values increased (as can be seen in Figure 13), possibly indicating a crack was initiating inside the zones of interest. Their initiation and total life were about 10000 and 30000 cycles respectively for the 610MPa test. For the 855MPa test it wasabout 3000 and 9000 cycles respectively, so standard surfaces give a initiation to total life ratio of 30%. The effect of the surface treatment appears to be that initiation life is extended. In the previous study [1] the thermography indicated 55% initiation life for a standard sample under 815MPa, which correspond to the smaller detected initiation crack sizes.

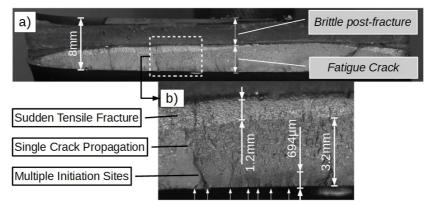Figure 13. T1 during full fatigue failure test of standard sample at 610MPa

Figure 14. Fracture face of 855MPa test a) full sample b) zoomed section

All the aforementioned fatigue phases are also represented in the crack surface photographs, where the measurements shown in Figure 14b) correspond to the results from the previous study [1]. This indicates that the fatigue life development is comparable so the initiation life ratios can also be compared. From Figure 5c) it is clear that the initiation starts on different planes at the surface and that those either meet deeper into the material (as in Figure 14b) at the start of the propagation zone) or are arrested as the larger crack diverts the stress from the surface.

5   CONCLUSION

The IR thermographic methods evaluated in this study gave clear results. The fatigue limit was detected in much shorter tests than with other methods and it has been shown that the bending process lowers fatigue limit. The initiating cracks are detected where the FEA model predicts them to be. Detected cracks are about ten times smaller than previous results under the prevision that the detected harmonics deviation is large enough. Crack face microscopy revealed the multiple initiation-sites before tensile failure that the thermographic data indicated. The ratio of initiation to the total fatigue life is similar to the previous study for the peened sample but less for the standard sample indicating a smaller detected crack. All these results enforce the validity of the use of thermography for investigating fatigue behaviour, even under the complex stress multi-axiality inside the bend.

6   ACKNOWLEDGEMENTS

7   REFERENCES

[1]   R. H. Talemi, S. Chhith, W. De Waele, "Experiental and numerical study on effect of forming process on low cycle fatigue behaviour of high strength steel", Fatigue & Fracture of Engineering Materials & Structures, 2017, DOI: 10.1111/ffe.12625

[2]   S. Glodez, M. Knez, J. Kramberger, "Fatigue behaviour of High Strength Steel S1100Q", Advanced Engineering, 2, 143-152, 2007

[3]   G. La Rosa, C. Clienti, F. Lo Savio, "Fatigue analysis by acoustic emission and thermographic techniques", Procedia Engineering, 74, 261-268, 2014.

[4]   J. Schijve, "Fatigue of Structures and Materials", Second Edition, Springer, ISBN-13: 978-1-4020-6807-2, p13-58, 2008

[5]   T. Ummenhofer, J. Medgenberg, "On the use of infrared thermography for the analysis of fatigue damage processes in welded joints", International Journal of Fatigue, 31, 130-137, 2009.

[6]   R. De Finis, D. Palumbo, U. Galietti, "Mechanical Behaviour of Stainless Steels under Dynamic Loading: An Investigation with Thermal Methods", Journal of Imaging, 2, 32, 2016

[7]   S. Chhith, W. De Waele, P. De Baets, "On-Line Detection of Fretting Fatigue Crack Initiation by Lock-In Thermography", International Symposium of Fretting Fatigue, 8, 2016.

[8]   O. Breitenstein, W. Warta, M. Langenkamp, "Lock-in Thermography: Basics and Use for Evaluating Electronic Devices and Materials", Second Edition, Springer, ISBN 978-3-642-02416-0, p14-22, 2010.

[9]   N. Micone, W. De Waele, "On the Application of Infrared Thermography and Potential Drop for the Accelerated Determination of an S-N Curve", Experimental Mechanics, 2016, DOI: 10.1007/s11340-016-0194-6